


Article

# Nature’s Wind Turbines: The Measured Aerodynamic Efficiency of Spinning Seeds Approaches Theoretical Limits

Timothy C.A. Molteno 

Department of Physics, University of Otago, P.O. Box 56, Dunedin, 9016, New Zealand; tim@physics.otago.ac.nz

**Abstract:** This paper describe a procedure to measure experimentally the power coefficient,  $C_p$ , of winged seeds, and apply this technique to seeds from the Norway maple (*Acer platanoides*). We measure  $C_p = 56.9 \pm 2\%$  at a tip speed ratio of  $3.21 \pm 0.06$ . Our results are in agreement with previously published CFD simulations that indicate that these seeds – operating in low-Reynolds number conditions – approach the Betz limit ( $C_p = 59.3\%$ ) the maximum possible efficiency for a wind turbine. In addition, this result is not consistent with the recent theoretical work of Okulov & Sørensen, which suggests that a single-bladed turbine with a tip-speed ratio of 3.2 can achieve a power efficiency of no more than 30%.

**Keywords:** Betz Limit; Aerodynamic Efficiency; Biomimicry

## 1. Introduction

Natural selection can lead to remarkable designs whose efficiency approaches fundamental limits. Biomimicry – using examples from the natural world to inspire solutions to engineering problems – has attracted interest in recent years as a means to design more efficient aerodynamic structures. For example, whale flukes [1,2] has have inspired designs for minimizing turbulence in turbine blades [3] and bumblebees have inspired flapping-wing flyers [4].

Winged seeds of some trees use a novel technique to increase their dispersal – and thus gain a competitive advantage. Shaped like small wings, they begin to spin as they fall, and the lift from this spinning slows their fall. Designs that are more efficient extract more energy from the air flow, fall more slowly and this increases the likelihood that they will land further from their parent tree, and thus increases their chances of surviving to adulthood.

Computational Fluid Dynamics (CFD) simulations have suggested [5,6] that these falling winged seeds (see Figure 1) have efficiencies that approach the Lanchester-Betz-Joukowski limit [7–9] – often regarded as the maximum possible efficiency for a wind turbine.

The Lanchester-Betz-Joukowski limit [10,11] hereafter “Betz limit”, states that no more than 59.3 % of the energy can be extracted from the wind by an un-shrouded wind turbine. This limit is considered optimistic, with more realistic modes that take into account effects like wake-rotation leading to lower limits, for example Glauert [12] showed the the optimal wind turbine efficiency depends on the tip-speed-ratio [10], the ratio,  $\lambda$ , of the speed of the tips of the turbine blades to the wind speed. for typical tip-speed ratios seen in wind turbines, the Glauert limit is below the Betz limit by about 20%. The best human-engineered wind turbines have efficiencies approaching 50% [11]. Recent theoretical work of Okulov & Sorensen [13] further explores the theoretical limits to turbine efficiency, and concludes using vortex theory, that a single-bladed turbine with a tip-speed ratio of 3.2 can achieve a power efficiency of no more than 30%.

This paper described an experimental procedure to measure directly the efficiency of falling seeds as wind-turbines. We then apply this technique to seeds of the Norway Maple (*Acer platanoides*), and find that our measurements are in broad agreement with previous

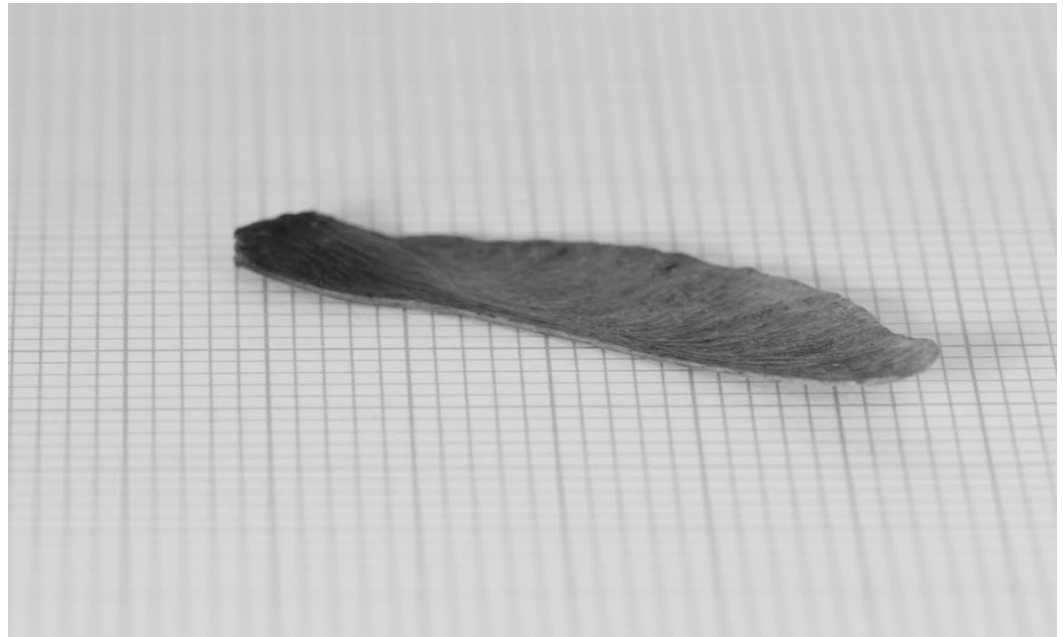


**Figure 1.** A winged seed from the Norway maple (*Acer platanoides*). The major grid spacing is 1cm.

numerical studies [6], and that the seeds have efficiencies that approach the Betz limit, and significantly exceed the theoretical limits derived by Okulov & Sorensen.

## 2. Theoretical limits on efficiency

Once the falling seed has settled into its spinning motion, it falls towards the ground with a constant velocity  $v_1$ . In this situation, the net upward aerodynamic force  $F_a$ , is balanced by the downward forces due to gravity.

$$F_a = F_g \equiv mg, \quad (1)$$

where  $m$  is the mass of the seed, and  $g$  is the gravitational constant. Thus measuring the seed mass establishes the magnitude of the aerodynamic force  $F_a$ . Using axial momentum-theory we can then derive an expression for  $F_a$  in terms of some simplified parameters of the motion.

### 2.1. Axial-momentum theory

The simplest theoretical derivation of the Betz limit uses using a highly simplified model of flow called *axial momentum theory*. This model assumes that air is incompressible, there is no heat transfer (dissipation), and the flow in and out of the rotating seed is axial and of uniform velocity. This aerodynamic force  $F_a$  is produced by changing the momentum of the air as it flows past the seed. From the point of view of the seed, the air below the seed rushes upwards with a speed  $v_1$ , is slowed by the seed, so that above the seed, the air is still moving upwards, but more slowly (with velocity  $v_2 < v_1$ ).

It can be shown (See for example [11,14]) that the velocity at the seed,  $v$ , is exactly half-way between  $v_1$  and  $v_2$ . We use a factor  $a$  to describe how much the incoming speed,  $v_1$ , and outgoing speed,  $v_2$ , differ from the speed at the seed. The velocity before the seed is  $v_1$ , the velocity at the seed is  $v_1(1 - a)$  and the velocity after the seed is  $v_1(1 - 2a)$ , where  $a$  is the *axial induction factor*. This relationship between flow-tube area and flow speed shown in Figure 2.

The mass mass flow rate,  $\dot{m}$ , through an area  $A$  is,

$$\dot{m} = \rho A v \quad (2)$$

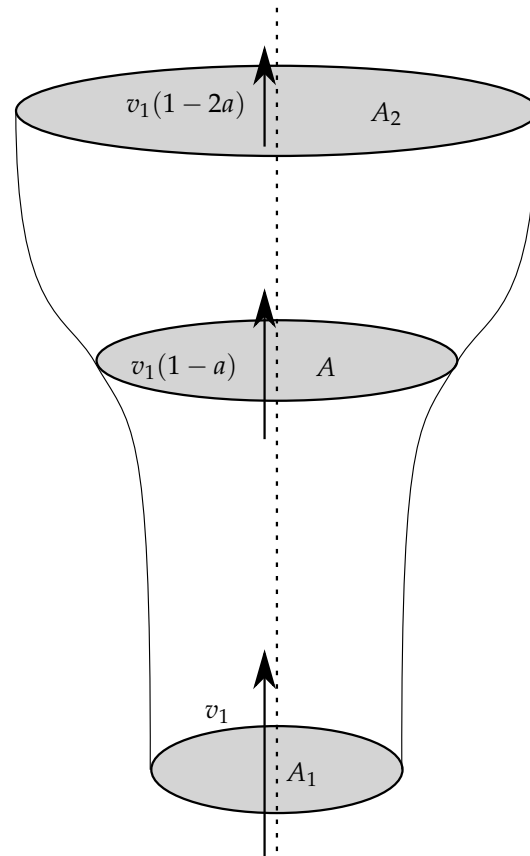


**Figure 2.** The flow tubes, before and after the falling seed. The wind approaches the disk of the seed with velocity  $v_1$ , and then slows down to velocity  $v_1(1-2a)$  in the tube after the seed. At the seed, the velocity is half-way between  $v_1(1-a)$ .

where  $A$  is the area,  $v$  is the velocity and  $\rho$  is the density. Conservation requires that  $\dot{m}_1 = \dot{m} = \dot{m}_2$ . 62  
63

#### 2.1.1. The force on the seed 64

The aerodynamic force on the seed is the difference in the momentum of the air before the seed (per unit time), and after the seed. In other words,

$$F_a = \frac{dmv}{dt} = \dot{m}_1 v_1 - \dot{m}_2 v_2$$

Substituting in for the mass-flow-rate (Equation 2) and using the axial induction factor we get

$$F_a = 2Aa\rho v_1^2(1-a) \quad (3)$$

We can rearrange Equation 3 to get

$$a(1-a) = \frac{F_a}{2A\rho v_1^2} \quad (4)$$

we can measure everything on the right-hand side of this equation. Substituting the known force for  $F_a$ , (Equation 1) we define  $c$  to be:

$$c \equiv \frac{F}{2A\rho v_1^2} = \frac{mg}{2A\rho v_1^2} \quad (5)$$

Equation 4 is then a quadratic equation for  $a$

$$a^2 - a + c = 0 \quad (6)$$

involving experimentally measurable quantities. Solving we get an expression for  $a$

$$a = \frac{1 \pm \sqrt{1 - 4c}}{2} \quad (7)$$

or

$$a = \left[ \frac{1}{2} - \frac{\sqrt{A\rho v_1^2 - 2F}}{2v_1\sqrt{A\rho}}, \quad \frac{1}{2} + \frac{\sqrt{A\rho v_1^2 - 2F}}{2v_1\sqrt{A\rho}} \right]$$

There are two solutions for  $a$ . However only one of these is physically possible –  $a$  must be less than 0.5, or the velocity after the seed is negative. This is

$$a = \frac{1}{2} - \frac{\sqrt{A\rho v_1^2 - 2F}}{2v_1\sqrt{A\rho}} \quad (8)$$

If  $a$  is known we can calculate the power using the force from Equation 3. The power becomes:

$$P = 2Aa\rho v_1^3(a - 1)^2 \quad (9)$$

### 2.1.2. The Power-coefficient

The maximum possible energy that could be extracted from a wind-turbine in an interval  $\Delta t$ , is limited by the kinetic energy  $U_k$  of the air with mass  $m_1$ , flowing with velocity  $v_1$ ,

$$U_k = \frac{1}{2}m_1v_1^2, \quad (10)$$

If the air flows through the turbine in  $\Delta t$ , the mass becomes  $m_1 = \dot{m}\Delta t$ , and where  $\dot{m}$  is the mass flow rate given in Equation 2. The kinetic energy is then

$$U_k = \frac{1}{2}\dot{m}\Delta t v_1^2 = \Delta t \frac{A\rho}{2}v_1^3,$$

and the maximum possible power  $P_{limit}$ , is

$$P_{limit} = \frac{U_k}{\Delta t} = \frac{A\rho}{2}v_1^3$$

The power coefficient  $C_p$  is the ratio of the power to the maximum possible power. It is given by:

$$C_p = \frac{P}{P_{limit}} = 4a(a - 1)^2 \quad (11)$$

where  $P$  has been substituted from Equation 9. To find the maximum possible  $C_p$ , differentiate to get

$$\frac{dC_p}{da} = 4(a - 1)(3a - 1).$$

This has two solutions  $a = 1$ , a minimum, and  $a = \frac{1}{3}$  which maximises  $C_p$  to be  $\frac{16}{27} \sim 0.593$ . This is the Lanchester–Betz–Joukowski limit [15], the maximum possible power efficiency for a wind turbine.

### 2.2. Refined Limits based on Vortex Theory

The Betz limit is derived assuming axial-momentum theory. Subsequent analyses have attempted to derive upper limits to efficiency based on more realistic models that take into account effects such as wake rotation.

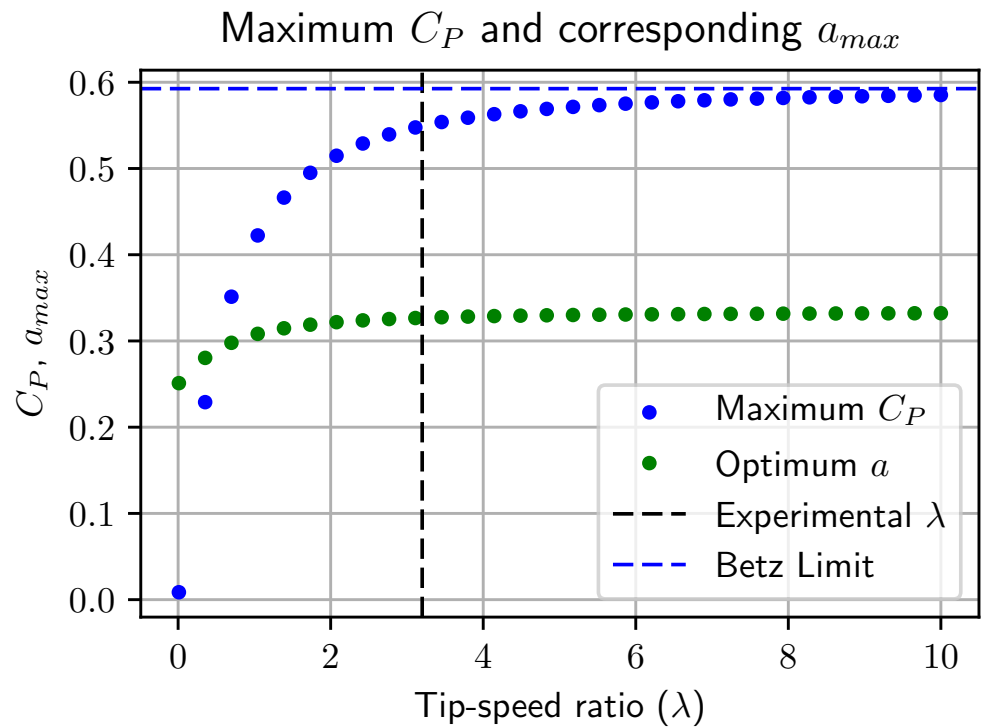


**Figure 3.** Glauert limits for an optimum wind maximum turbine as a function of tip-speed-ratio. The axial induction factor that maximises  $C_p$  is shown as  $a_{max}$ , as well as the maximum  $C_p$ . At large tip-speeds,  $C_p$  converges to the Betz limit, and the axial induction factor converges to  $a = \frac{1}{3}$ .

Glauert [12] developed such a model - assuming an infinite number of blades, and showed that the optimum efficiency should be a function of the tip-speed ratio. The Glauert limit approaches the Betz limit for large tip-speed ratios  $\lambda \gg 10$ , and approaches zero as the tip-speed ratio approaches zero (see Figure 3). Recently [16] a closed-form expression for the  $C_p$  under these assumptions was derived:

$$C_p = \frac{1}{\lambda^2} (a-1) \left( 8a^2(a-1)^2 \log \left( \frac{\lambda + \sqrt{-4a(a-1) + \lambda^2}}{2\sqrt{-a(a-1)}} \right) + \lambda \left( \lambda^3 + \sqrt{-4a(a-1) + \lambda^2} (2a(a-1) - \lambda^2) \right) \right).$$

Several further limits have been suggested (see [13,17] for more details). Most indicate limits lower than the Betz limit, however some imply that in the limit that the number of blades tend to infinity and the tip speed ratio is large, provide upper limits that exceed the Betz limit.

### 3. Experimental Methods

Substituting for  $a$  from Equation 8 into the expression for  $C_p$  (Equation 11), yields an expression for  $C_p$  in terms of measurable quantities.

$$C_p = 4a(a-1)^2 = \frac{F}{A\rho v_1^2} + \frac{F}{A^{\frac{3}{2}}\rho^{\frac{3}{2}}v_1^3} \sqrt{A\rho v_1^2 - 2F}. \quad (12)$$

The only parameters required to determine  $C_p$  are,  $A$ ,  $\rho$ ,  $v_1$  and  $F = mg$ .

This suggest an experimental procedure for calculating  $C_p$ . The equation for  $C_p$  (Equation 12) depends only on the following quantities:

- mass  $m$  of the seed,
- swept area,  $A$ , of the seed,
- falling terminal velocity  $v_1$ ,
- density of air  $\rho$ .

The equipment needed to measure these is relatively straightforward – a diagram of a suitable setup is shown in Figure 5. A balance is required to measure seed mass, and video capture is used measure the terminal velocity  $v_1$ , and the center of rotation.

### 3.1. Characterization of Experimental Uncertainty

When a quantity is not precisely known, for example, if the quantity is based on a measurement, then we will characterize the quantity as a probability distribution. The swept radius of the seed  $r$  is measured to be 38mm with an uncertainty of 0.5 mm. In this case the we can choose to represent this quantity as  $U(37.5, 38.5)$  – a uniform probability distribution between 37.5 and 38.5.

The swept area  $A = \pi r^2$  can be calculated algebraically, or simulated by evaluating the function (in this case  $\pi r^2$ ) drawing values for  $r$  from  $U(37.5, 38.5)$ . Figure 4 shows the histogram of area values sampled from  $r \sim U(37.5, 38.5)$ .

Note that the median of the area distribution is not equal to the area calculated from the median of the radius distribution as the are is a nonlinear function of the radius.

### 3.2. Falling Velocity Measurement

The horizontal camera films the vertical motion of the seed, and the time is measured (by counting frames) from the moment the seed intersects a laser level line (point  $p$  in Figure 5) until it touches the floor, (point  $q$  Figure 5). In the setup described here, this distance was  $1.270 \text{ m} \pm 2\text{mm}$ . To capture the uncertainty in this measurement, it is represented by a normal distribution with a mean of 1.27 m and a standard deviation of 2 mm ( $N(1.27, 0.002)$ ). With a frame-rate of 100 FPS, this took  $134 \pm 1$  frames (represented by a uniform distribution  $U(133, 135)$ ). This resulted in a falling velocity,  $v_1$  distribution of

$$v_1 = 0.9478 \pm 0.007 \quad (13)$$

### 3.3. Swept Area Measurement

The upward-looking camera is used to measure the axial rotation period of the spinning seed, as well as determining the center of rotation of the seed, and from this the area of the rotor. A still image showing the approximate center of rotation is shown in Figure 6. From this center of location, the span is measured as the distance to the rotor tip  $r_s$ , and the swept area  $A = \pi r_s^2$

### 3.4. Air Density

The air density is calculated from the measured temperature, relative humidity and atmospheric pressure. This is done in two stages, first calculating the saturation pressure  $P_s$  using Tetens's formula [18].

$$P_s = 6.1078 e^{\frac{17.9 T_c}{T_c + 237.3}}$$

where  $T_c$  is the temperature in Celsius. The partial pressure of water vapour  $p_v$  is then given by  $p_v = \phi P_s$  where  $\phi$  is the measured relative humidity. The partial pressure of dry air is then  $P_d = P_a - P_v$ , where  $P_a$  is the atmospheric pressure. The ideal gas equation, coupled with the molar mass of water vapour and dry air, gives the air density

$$\rho = \frac{P_d M_d}{RT} + \frac{P_v M_v}{RT} \quad (14)$$

where  $R = 8.314$  is the universal gas constant, and  $T$  is the air temperature in Kelvin.

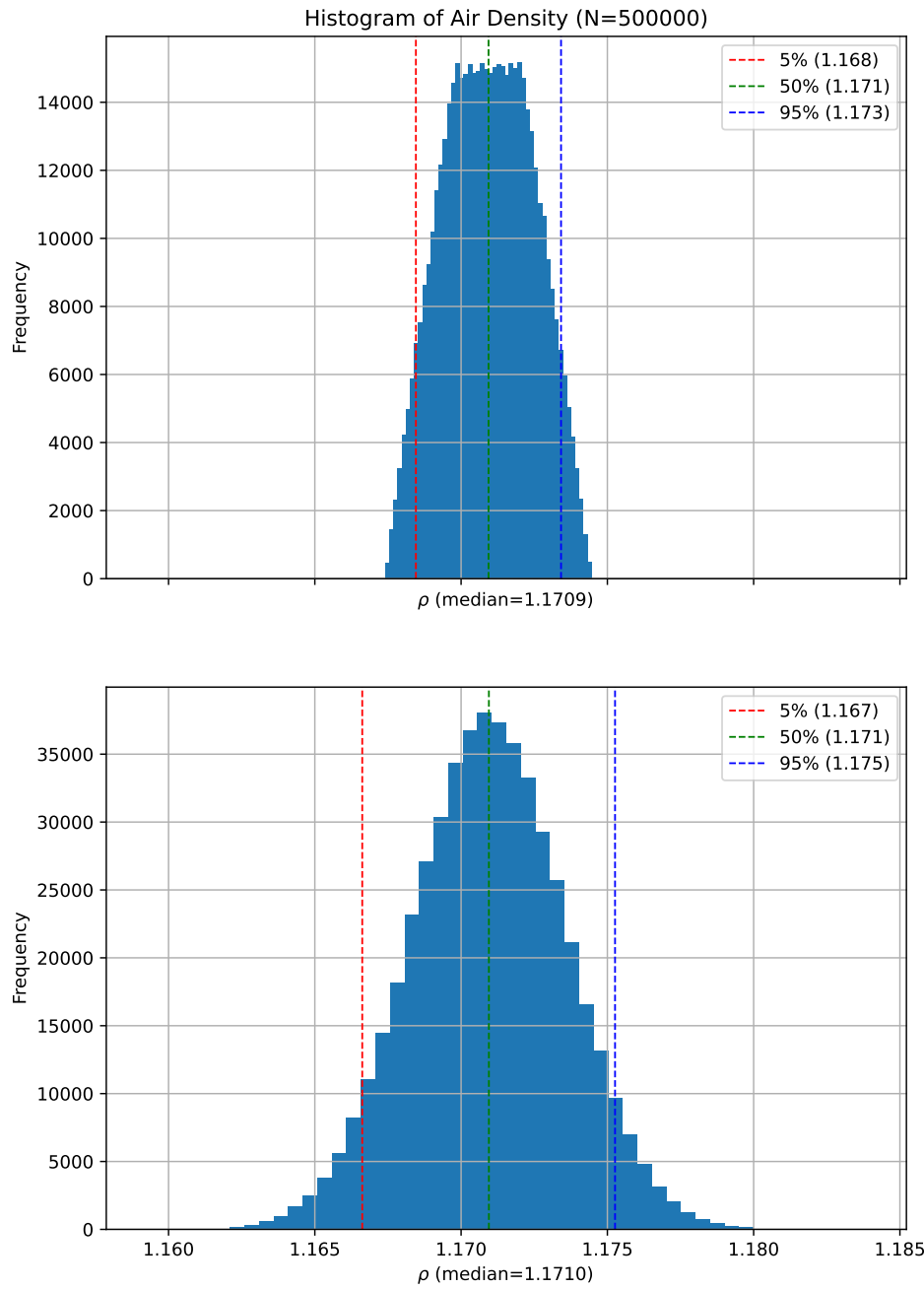


**Figure 4.** Histogram of air density values calculated with different uncertainties for temperature, humidity and air-pressure. In the top plot, the uncertainties are uniform distributions, and in the lower one, they are Gaussian distributions. The median, and 5-95% ranges are not significantly changed by these different choices.

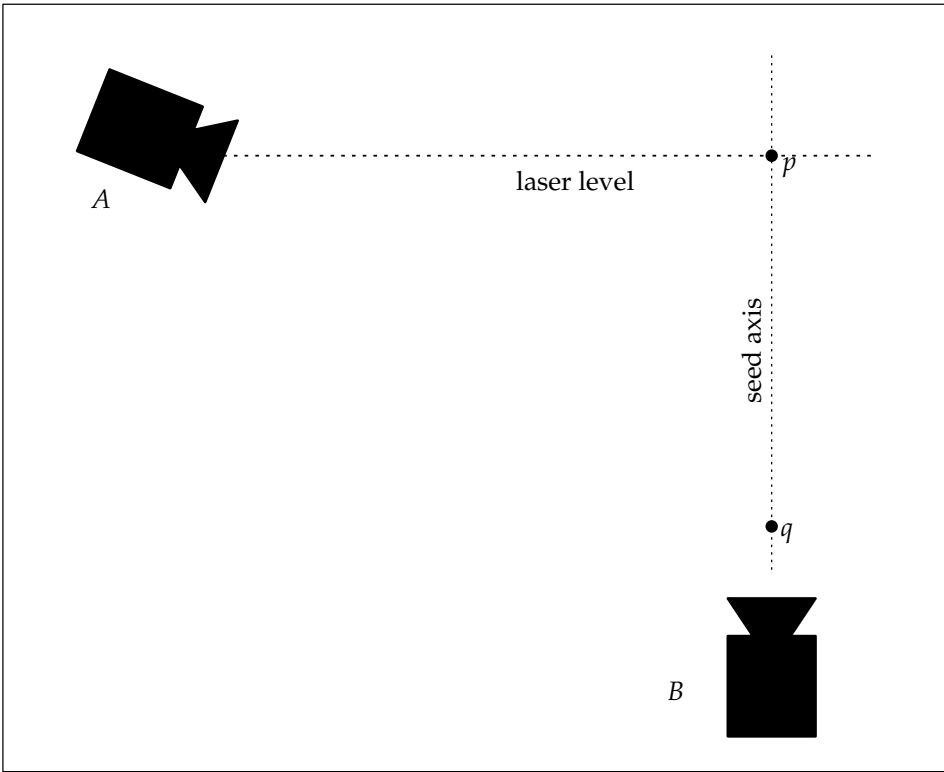


**Figure 5.** Diagram of apparatus for measuring seed turbine efficiency. Camera *A* looking horizontally, is used to determine the terminal falling speed, while camera *B* looking upwards, is used to measure the center of rotation, and hence the swept area *A*.

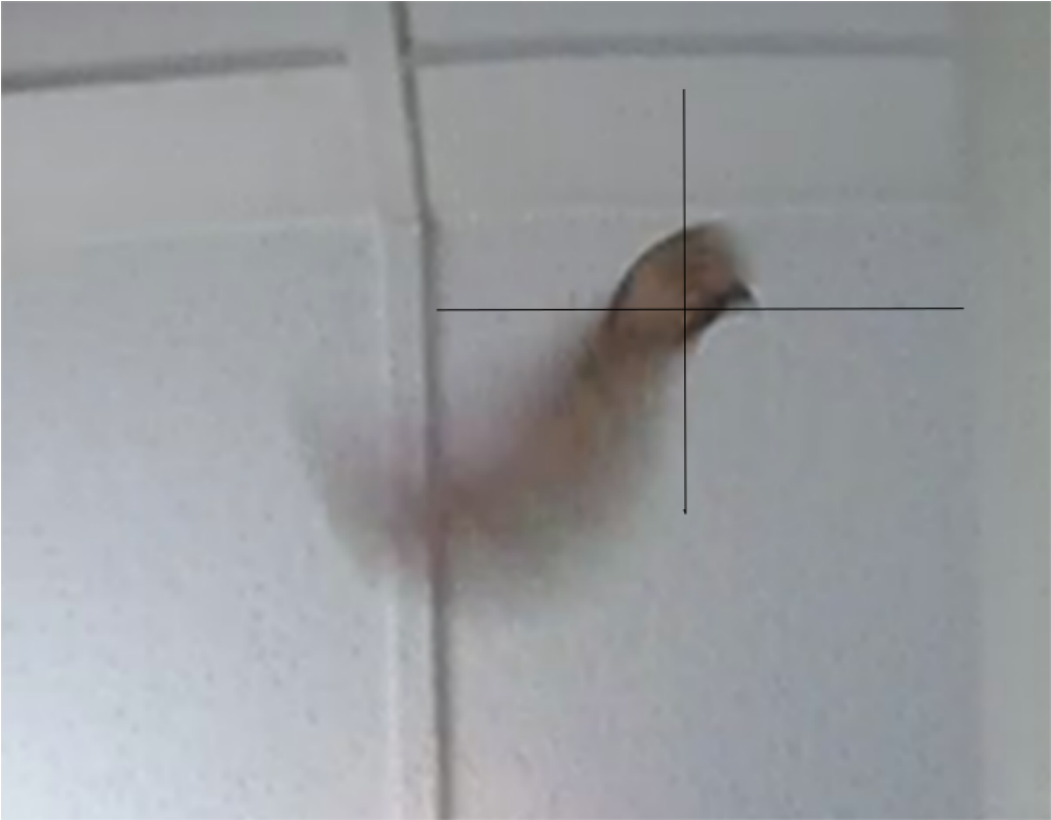


**Figure 6.** Still image from the upward looking camera used to estimate the centre of rotation. The approximate center of rotation is shown by the cross-hairs.



4. Results

The experimental procedure described in the previous section was applied to a seed rotor shown in Figure 1. Each measurement had an associated uncertainty, these are shown in Table 1. The mass  $m$  was measured using a Mettler digital balance as 0.19g with an uncertainty of 0.01g. Its measured value is represented as a uniform distribution between 0.18 and 0.20 grams denoted by  $U(0.18,0.20)$ .

**Table 1.** Experimental parameters measured from a falling Norway maple seed. Uncertainties are expressed as probability distributions.

Quantity	Units	Symbol	Uncertainty
mass	g	$m$	$U(0.18, 0.20)$
Rotation Frequency	Hz	$f$	$12.744 \pm 0.12$
Falling speed	$ms^{-1}$	$v_1$	$0.9478 \pm 0.007$
Tip Speed	$ms^{-1}$		$3.0429 \pm 0.05$
Tip Speed Ratio		$\lambda$	$3.211 \pm 0.033$
Reynolds Number		$R$	$2042.6 \pm 22.5$
Swept radius	mm	$r$	$U(37.5, 38.5)$
Swept area	$m^2$	$A$	$0.004537 \pm 0.0001$
Air Temperature	C	$T$	$N(23.9, 0.3)$
Relative Humidity	%	$\phi$	$N(68.6, 1.0)$
Air Density	$kgm^{-3}$	$\rho$	$1.17092 \pm 0.004$

Using the measured values from Table 1, the falling speed calculation results in a best estimate of  $0.9478\ ms^{-1}$ , and explicitly incorporating uncertainty represented by  $0.9478 \pm 0.007$ . The swept area calculation is the largest contributor of uncertainty to the final result. The location of the center of rotation is imprecise (with an uncertainty of 1mm  $U(37.5, 38.5)$ ), and the sweep radius is squared in order to calculate the area. The result is  $A \sim 0.004537 \pm 0.0001\ m^2$ .

By sampling from the distributions of parameters a histogram of  $C_p$  values can be calculated, this is shown in Figure 7. The best estimate (median) of this distribution is 56.93 %. 90 percent of this distribution lies between 54.6 and 59.3 %. Thus the measured power coefficient of the seed studied can be stated as  $C_p = 56.9 \pm 2.4\%$ .

4.1. Tip Speed Ratio

Glauert’s computations of optimum turbine efficiency taking wake rotation losses into consideration [13], indicate that the efficiency of an optimum turbine is lower than the Betz limit at low tip speed ratios. The measured tip speed,  $\lambda = \omega r$  was  $3.0426 \pm 0.05$ . This gives a tip speed ratio of  $3.21 \pm 0.03$ .

For the tip speed ratios in the region of 3.2, the optimum turbine efficiency is approximately 90% of the Betz limit, or 53.3%. The results shown in Figure 7 indicates that approximately 0.36% of simulated  $C_p$  values lie below this Glauert limit. It is highly likely ( $\geq 99\%$ ) that the efficiency of the seed rotor exceeds the Glauert limit.

5. Discussion and Conclusion

The analysis presented here is based on easily performed measurements on falling seeds. The results confirm that Norway-maple seeds are remarkably efficient with a power-coefficient measured to be  $C_p = 0.569 \pm 0.024$ . This measurement is in agreement with CFD predictions [6]. Analysis of experimental uncertainties show that there is a  $\sim 4.8\%$  of chance that the measured  $C_p$  value exceeds the Betz limit.

The measured tip-speed ratio is relatively low at  $3.21 \pm 0.06$ . Glauert, taking wake rotation into account, derived a limit for turbine efficiency that for a tip speed ratio of 3.2 is 54.94 %. Our results show that it is 92% likely that the efficiency of a falling Norway-maple seed exceeds the Glauert limit.

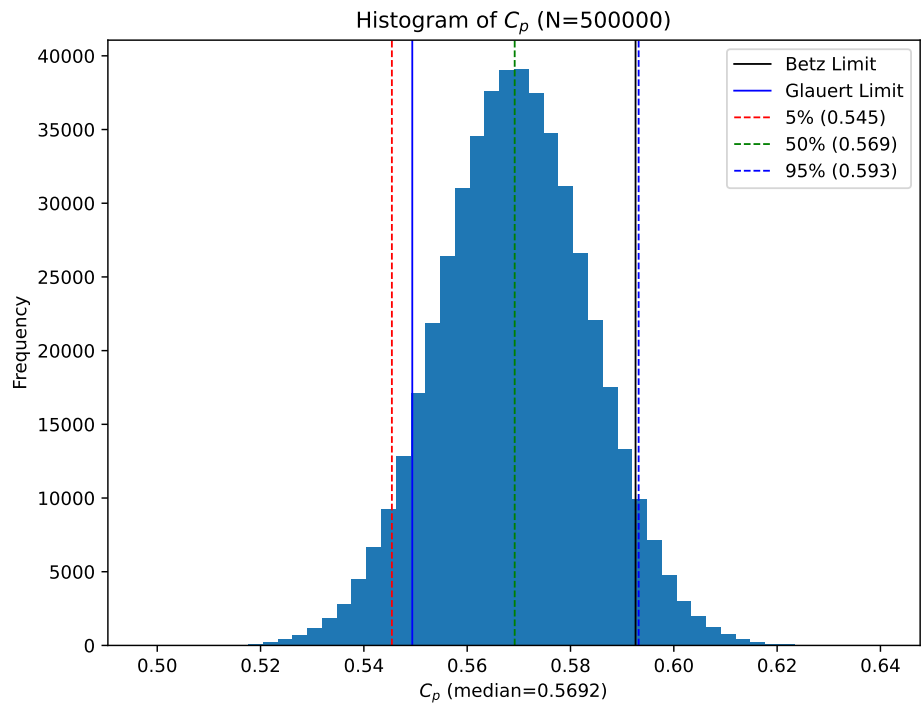


**Figure 7.** Histogram of 500000 randomly generated  $C_p$  values for a single seed, showing the experimental uncertainty for the estimate of  $C_p$ . The Betz limit is shown as the black dotted line close to the 95th percentiles of the  $C_p$  distribution. For this seed, 95% of  $C_p$  values lie in the range  $0.569 \pm 0.023$ .

Recent treatments have refined the Betz limit (see for example [13]) taking into consideration the finite number of blades as well as wake rotation. Okulov and Sorensen [13] find that with a tip-speed ratio of 3.2, the maximum a single-bladed turbine can only extract 30% of the available energy. The results we obtain ( $C_p = 0.569 \pm 0.024$ ) far exceed this limit.

Modern large wind turbines achieve peak values for  $C_p$  in the range of 0.45 to 0.50,[2] about 75% to 85% of the theoretically possible maximum. The falling seed achieves  $\sim 95\%$  of the Betz limit, a remarkable result, and in agreement with the CFD predictions of Holden et al. [6].

The upper limit on the amount of energy that can be extracted from air-flow by any device with projected area  $A$ , is usually given as the total kinetic energy contained in the wind that passes *through* the area  $A$  (see Equation 2). This neglects the possibility that a wind-turbine has an effect on the air outside its projected area. It is quite likely, at very low Reynolds numbers, that this does not hold true. Thus for very low Reynolds number flows, it is possible, at least in principle, for the power extracted from the air by the turbine to exceed the maximum kinetic energy in the wind passing through the projected area, i.e, for  $C_p$  to exceed 1.0. Therefore, one possible explanation of our experimental results is that in our scenario, the influence of the flow around the object does extend far beyond the projected area of the object itself, and therefore the limit for  $P_{max}$  in Equation 10 is artificially low.

**Funding:** This research received no external funding

**Institutional Review Board Statement:** Not applicable

**Informed Consent Statement:** Not applicable

**Data Availability Statement:** Not applicable

**Conflicts of Interest:** The author declares no conflict of interest.

Symbols

The following symbols are used in this manuscript:

- $C_p$  Power coefficient (Equation 11)
- $q$  Axial induction factor
- $\rho$  Air density
- $F_a$  Aerodynamic force

References

1. Sirohia, J. Microflyers: inspiration from nature. In Proceedings of the Proc. of SPIE Vol, 2013, Vol. 8686, pp. 86860U–1.

2. Miklosovic, D.; Murray, M.; Howle, L.; Fish, F. Leading-edge tubercles delay stall on humpback whale (Megaptera novaeangliae) flippers. *Physics of fluids* **2004**, *16*, L39–L42.

3. Fish, F.E.; Weber, P.W.; Murray, M.M.; Howle, L.E. Marine applications of the biomimetic Humpback whale flipper. *Marine Technology Society Journal* **2011**, *45*, 198–207.

4. Thompson, M.J.; Burnett, J.; Ixtabalan, D.M.; Tran, D.; Batra, A.; Rodriguez, A.; Steele, B. Experimental Design of a Flapping Wing Micro Air Vehicle through Biomimicry of Bumblebees. In Proceedings of the AIAA Infotech @ Aerospace, 2015, p. 1454.

5. Yung-Jeh, C. A new biomimicry marine current turbine: Study of hydrodynamic performance and wake using software OpenFOAM. *Journal of Hydrodynamics, Ser. B* **2016**, *28*, 125–141.

6. Holden, J.R.; Caley, T.M.; Turner, M.G. Maple Seed Performance as a Wind Turbine. In Proceedings of the 53rd AIAA Aerospace Sciences Meeting, 2015, p. 1304.

7. Joukowsky, N. Vortex theory of screw propeller, I. *Trudy Otdeleniya Fizicheskikh Nauk Obshchestva Lubitelei Estestvoznaniya* **1912**, *16*, 1–31.

8. Lanchester, F.W. A contribution to the theory of propulsion and the screw propeller. *Journal of the American Society for Naval Engineers* **1915**, *27*, 509–510.

9. Betz, A. Das maximum der theoretisch moglichen Auswendung des Windes durch Windmotoren. *Zeitschrift fur gesamte Turbinewesen* **1920**, *26*.

10. Ragheb, M.; Ragheb, A.M. *Wind turbines theory – the Betz equation and optimal rotor tip speed ratio*; INTECH Open Access Publisher, 2011.

11. Hansen, M.O. *Aerodynamics of wind turbines*; Routledge, 2015.

12. Glauert, H. Airplane propellers. In *Aerodynamic theory*; Springer, 1935; pp. 169–360.

13. Okulov, V.L.; Sørensen, J.N. Refined Betz limit for rotors with a finite number of blades. *Wind Energy* **2008**, *11*, 415–426.

14. Eggleston, D.M.; Stoddard, F. *Wind turbine engineering design*; Van Nostrand Reinhold Co. Inc., New York, NY, 1987.

15. Van Kuik, G.A. The Lanchester–Betz–Joukowsky limit. *Wind Energy* **2007**, *10*, 289–291.

16. Sørensen, J.N.; van Kuik, G.A. General momentum theory for wind turbines at low tip speed ratios. *Wind Energy* **2011**, *14*, 821–839.

17. Okulov, V.L.; Sørensen, J.N. Maximum efficiency of wind turbine rotors using Joukowsky and Betz approaches. *Journal of Fluid Mechanics* **2010**, *649*, 497–508.

18. Dilley, A. On the computer calculation of vapor pressure and specific humidity gradients from psychrometric data. *Journal of Applied meteorology* **1968**, *7*, 717–719.